

Brain-actuated Humanoid Robot Navigation Control using Asynchronous Brain-Computer Interface

Yongwook Chae, Sungho Jo, Member, IEEE and Jaeseung Jeong, Member, IEEE

Abstract—Brain-actuated robotic systems have been proposed as a new control interface to translate different human intentions into appropriate motion commands for robotic applications. This study proposes a brain-actuated humanoid robot navigation system that uses an EEG-BCI. The experimental procedures consisted of offline training sessions, online feedback test sessions, and real-time control sessions. During the offline training sessions, amplitude features from the EEGs were extracted using band power analysis, and the informative feature components were selected using the Fisher ratio and the linear discriminant analysis (LDA) distance metric. The Intentional Activity Classifier (IAC) and the Motor Direction Classifier (MDC) were hierarchically structured and trained to build an asynchronous BCI system. During the navigation experiments, the subject controlled the humanoid robot in an indoor maze using the BCI system with real-time images from the camera on the robot's head. The results showed that three subjects successfully navigated the indoor maze using the proposed brain-actuated humanoid robot navigation system.

I. INTRODUCTION

A Brain-Computer Interface (BCI) system has been devised to translate different mental states into appropriate commands. From a clinical viewpoint, electroencephalography (EEG)-based BCIs have received increasing interest because they are easier to record and are associated with less risks compared to other more invasive BCI systems [1], [2]. Recent studies have demonstrated the feasibility of EEG-based brain-actuated devices, such as mobile robots, neuroprosthetics, wheelchairs and humanoid robots [3], [5]-[7].

The first example of these devices was a mobile robot that was developed by Millan et al. [1]. They applied an asynchronous BCI protocol and a band power analysis method as the feature extraction method. To improve the stability and accuracy of the system, they employed a state-dependent

agent-based model. In that study, human subjects successfully moved a robot between several rooms by mental control.

Another interesting type of the brain-actuated device is the wheelchair navigation system [3], [4]. Recently, Iturrate et al. [3] proposed a new brain-controlled wheelchair that uses a P300-based protocol and an automated navigation system. Because the proposed wheelchair can avoid obstacles by using a laser scanner, the user is only required to focus on the desired direction of movement using the interface system that displays a real-time virtual reconstruction of the environment. They demonstrated that all of the subjects were able to successfully operate the device.

Among the various brain-actuated devices, the humanoid robot control system has been highlighted because humanoid robots can perform more varied and complicated actions and their motions are similar to those of humans. The first brain-actuated humanoid robot that used EEG-BCI was attempted by Bell et al. [5]. In that study, the user selected a target box that was between a green box and a red box based on the detection of P300 signals, and a Fujitsu HOAP-2 humanoid robot conveyed the box to a pre-defined location. Although the results demonstrated successful control of the humanoid robot, there were some limitations: 1) the robot motions were pre-programmed and were limited to the two selective choices (i.e., the two boxes), and 2) the timing of the motion commands was controlled by the system, not by a user.

Based on the previous studies, many systems employed obstacle avoidance or the agent-based model to enhance the performance on navigation tasks. The low information transfer rate (20-30 bits/min) and the limited control capacities make it difficult to use in a complex tasks [6]. Meanwhile, these systems were designed as a menu-based system using the P300-based protocol, and because of this characteristic, the controllability based on state-dependent conditions, such as the perceptual states of an encountered environment, and the number of choices of a menu-based system is restricted.

This study proposes a novel brain-actuated humanoid robot navigation system that allows direct-control so that the users to can select low-level motion primitives (e.g., "stop", "forward walk", "body turn", "left head turn", and "right head turn") instead of high-level motion primitives (e.g., go to the limited target place) in the menu-based system. To implement a direct-control system, a band power based BCI system was used to extract the low-level commands from the user's intention (e.g., left hand, right hand and foot). This feature differs from previous P300-based humanoid robot control systems, which used limited targets and high-level commands [5], and it enables the user to control the robot in more varied angles of motion. In addition, the system employed the asynchronous paradigm. Since an asynchronous BCI system has no global cues: instead, it continuously detects not only the intentional-control (IC) states (e.g., motor imagery) but also non-control state (NC, formerly called idling state), it enables

Manuscript received March 4, 2011. This work was supported by the Chung Moon Soul Research Center for Bio Information and Bio Electronics in KAIST, KAIST High Risk High Return Project, the Korea government (MEST) under the KRF grant (No.2010-0015226), the Korea Science and Engineering Foundation grant funded by the Korea government (grant numbers R01-2007-000-21094-0, M10644000028-06N4400-02810; grant numbers 20090093897, 20090083561)

Jaeseung Jeong is with Department of Bio and Brain Engineering, Korea Advanced Institute of Science and Technology, 291 Daehak-ro, Yuseong-gu, Daejeon, South Korea (co-corresponding author to provide phone: +82-42-869-4359; fax: +82-42-869-4310; e-mail: jsjeong@kaist.ac.kr)

Sungho Joe is with Department of Computer Science, Korea Advanced Institute of Science and Technology, 291 Daehak-ro, Yuseong-gu, Daejeon, South Korea (co-corresponding author to provide phone: +82-42-350-3540; e-mail:shjo@cs.kaist.ac.kr)

Yongwook Chae is with Department of Bio and Brain Engineering, Korea Advanced Institute of Science and Technology, 291 Daehak-ro, Yuseong-gu, Daejeon, South Korea (e-mail:chaeyw82@gmail.com).

user to regulate the timing of control and shows higher ITR than synchronous system [10]-[12]. To enrich the control capacity of the navigation system, the control paradigm was designed to enable the user to select five different motions, such as left or right head spin, left or right turning walk, or a straight walk, using just three motor commands based on the postural dependent states. This approach creates a successful navigation system that enables the user to navigate the indoor maze using the humanoid robot.

II. METHODS

The system consisted of three sub-systems: the BCI system, the interface system, and the control system. During the three main procedures (offline training, online feedback testing, and real-time control), the system processed three different types of data, (i.e., sensed visual information, measured EEG signals, and motion commands).

A. Training Protocol

During the offline training sessions, subjects were asked to imagine the motor imagery (MI) tasks, which were referred to as “left hand imagery”, “right hand imagery”, and “foot imagery” or were asked to stay in the Non-Control (NC) state referred to as “rest”. The subjects were instructed to select one side of the foot consistently during the entire experiment to prevent confusion. During the first two days, the subject underwent three offline training sessions per day. Each session consisted of 20 trials per task, and the interface system provided training cues on the interface monitor as illustrated in Fig. 1.A. During each session, nothing happened for the first 2 s. Then, the first text cue (e.g., “rest”) with a solid circle appeared in the center of screen. After 4 s, a cue with the target arrows and the related text appeared to indicate

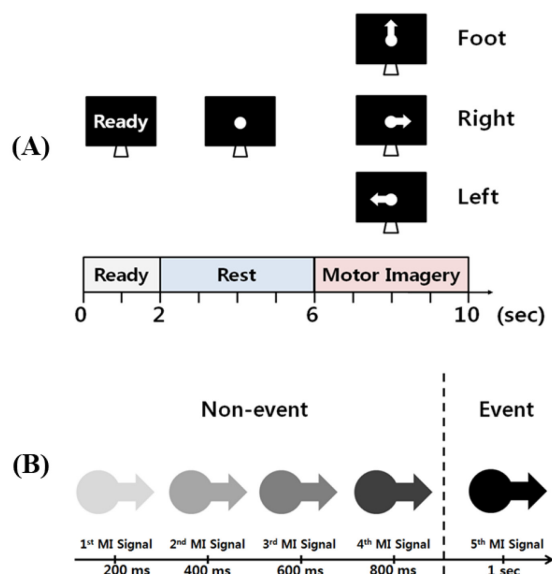


Fig. 1. A) Training protocol: after the ready and rest sessions, the subject was asked to imagine a motor imagery indicated by a cue B) Fading feedback rule was used to secure a robust classification of a mental state from the ongoing EEG.

one of the MI tasks. To prevent forecasting, the presentation order of the cues was block randomized. After each offline training session, the BCI system 1) analyzed the collected EEG data to extract the appropriate features, 2) selected the informative feature components, and 3) trained two hierarchical classifiers based on the selected feature components.

During the online feedback test, the interface system displayed a target cue and a classified mental state using the fading feedback rule. After the first two days of the offline training sessions, subjects repeated an online feedback test run and an offline training run until the hit ratio of the online test run was greater than 75%. Each feedback test run consisted of 15 trials per task. The NC and MI states of each trial lasted for 6 s. Its presentation order was also block randomized.

B. Experimental Setup

Three healthy male subjects (right handed, age 26.3 ± 3.1 yr) participated in the experiments. They had not participated in any prior BCI experiments. They were required to navigate from a departure point to a destination point in the indoor maze via five waypoints as Fig. 2 illustrated. The maze measured 1.5 m (width) by 3 m (length). A circled number of front waypoints and the arrows of guided direction were denoted on the walls and the user was able to check these guide signs using the interface system. To become familiar with the control system, each subject underwent an open trial for fifteen minutes before the main experiments. They participated in all of the sessions to test the real-time control scenario as follows. The subjects were able to obtain information on the robot states and their mental states through the interface system. A camera on the robot acquired visual images at 5 frames per sec. The mental states from the fading feedback system were updated every 250 msec. Each subject had access to the robot state and the mental state information on the PC screen using the interface system. Each subject controlled the robot three times using the proposed BCI system and one time using keyboard keystrokes for comparison. During the manual keyboard control, each subject was asked to drive the robot using three keys: up, right, and left. The manual session was performed prior to the BCI

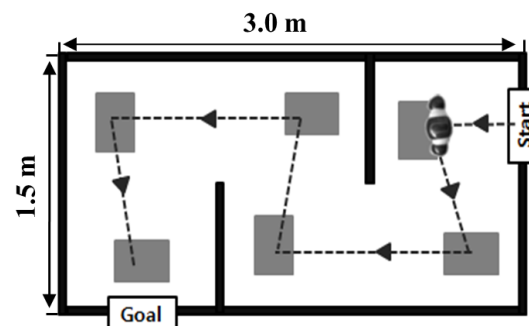


Fig. 2. Objective of the navigation task was to depart the start area and to arrive at the goal area by passing the five waypoints.

control sessions.

C. Data Acquisition

During the experiments, the EEG signals of a subject were recorded at a sampling rate of 250 Hz from 21 electrodes (F3, Fz, F4, FT7, FC3, FCz, FC4, FT8, T7, C3, Cz, C4, T8, TP7, CP3, CPz, CP4, TP8, P3, Pz, and P4 see Fig.3.). The sampled EEG signals from 9 channels (FC3, FCz, FC4, C3, Cz, C4, P3, Pz and P4) were spatially filtered with the large Laplacian filter [2], [7]. Every 250 ms, the amplitudes in the 4-36 Hz band was estimated over the last two seconds (i.e., 500 samples) using an autoregressive frequency analysis [7] with a model order of 16. Therefore, in the offline training sessions, 32 amplitude feature vectors with 288 dimensions (9 channels multiplied by 32 frequency components in the 4-36-Hz band) were collected within the MI and Rest periods (4 sec) for each trial. These feature vectors were used to select the feature components and to train the classifiers. During the online tests and the real-time control sessions, the feature vectors were sampled every 250 ms from the selected feature components and were used to produce the real-time feedback and the classification of the motion commands.

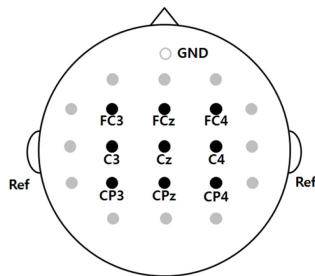


Fig. 3. EEG electrode positions with respect to the international 10-20 system. Electrode positions marked with gray circles are only used in computation of the spatial filter. The nine black circles indicate electrode positions used as main feature channels. All the electrodes are referenced to the left and right mastoids.

D. Feature Selection

To select informative feature components in the time-channel-frequency domain, the Fisher ratio [8] and the Linear Discriminant Analysis (LDA) [9], [10] were used. For the amplitude feature vector from the NC and MI states, let μ_{rest} and σ_{rest} denote the mean and variance, respectively, of the amplitude feature set from the “rest” state, and let μ_{MI} and σ_{MI} denote the mean and variance, respectively, of the amplitude feature set from the MI state. The Fisher ratio is defined as the ratio of the between-class variance to the within-class variance [8] as follows:

$$fr = \frac{\sigma_{between}^2}{\sigma_{within}^2} = \frac{(\mu_{rest} - \mu_{MI})^2}{\sigma_{rest}^2 + \sigma_{MI}^2} \quad (1)$$

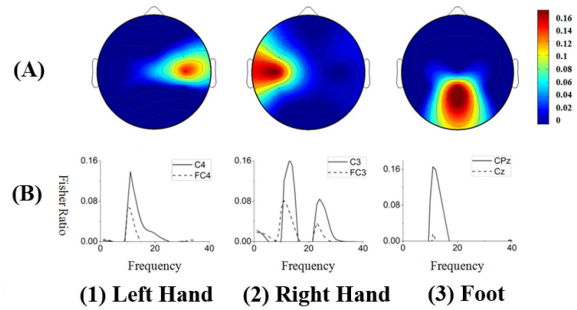


Fig. 4. Channel-frequency selection using the Fisher ratios from the three sets of “rest” vs. MI tasks. (A) Topographical distribution of the Fisher ratios of subject A. The Fisher ratios on the topological diagram were selected from the top-scoring frequencies of each set. The first two top-scoring channels for the “left hand imagery” tasks were channels C4 and FC4, channels C3 and FC3 were selected for the “right hand imagery” tasks, and channels CPz and Cz were selected for the “foot imagery” tasks. (B) Spectral distribution of the Fisher ratios for subject A. For the “left hand imagery” tasks, the maximum Fisher ratio of C4 was 0.15 at 12 Hz, and a 5-Hz window centered at 12 Hz was selected as the discriminative frequency region.

The Fisher ratio is a measure of the (linear) discrimination and the separability of the two variables, and it can also be considered as a signal-to-noise ratio. Among the channel-frequency pairs that were acquired from the EEG data of the two mental states (“rest” vs. each of the MIs), a channel-frequency pair with the highest Fisher ratio value was considered the most discriminative channel frequency pair. The corresponding channel and a frequency window of 5 Hz centered at the top-scoring frequency were selected as the most discriminative band. The amplitude value averaged over the window was designated as the first informative amplitude feature. For the second top-scoring channel in the Fisher ratio, the same procedure was applied to select the second informative amplitude feature.

To avoid any unintentional noisy periods, the informative time periods were determined for the NC and MI mental states by using a LDA classifier. The amplitude feature segments from the training trials between 2 s and 6 s were assigned to the NC class, and the signal segments between 6 s and 10 s are assigned to the MI class as illustrated in Fig. 4. The discriminant values were averaged over the time, and the 1-s intervals that were centered at the maximum and minimum LDA distance points were selected as the optimal MI period and the optimal rest period, respectively.

E. Classification

To translate the intended EEG data into its appropriate movement commands for the humanoid robot, the Intentional Activity Classifier (IAC) and the Movement Direction Classifier (MDC) were hierarchically employed. The IAC classifies between the NC and MI states. If the signals were interpreted as the MI state by the IAC, then the MDC classified the specific MI state as either “left-hand”, “right-hand”, or “foot” states.

Based on the feature selection method, the training feature

set for the IAC consisted of the informative amplitude features that were extracted from two of the most discriminative bands during the NC and MI periods. The Linear Discriminant Analysis (LDA) was used to train the feature sets for the IAC. As a result of the training, the negative output values denoted the NC classes, and the positive output values of the IAC denoted the MI classes. To find a suitable threshold that balances the true positives (TPs) and the false positives (FPs), a sample-by-sample receiver operator characteristic (ROC) analysis [11] was used. The two axes of the ROC curve consisted of the true positive rate (TPR) and the false negative rate (FPR). The points above the ROC curve were calculated from a given threshold. In this study, a balanced point was considered as a threshold that resulted in a TPR value that equals 1-FPR [11], and the threshold value on the point was used to redefine the IAC's threshold.

The informative amplitude features from the MI states during the MI period were used to train the MDC. When the IAC classified a feature into an MI class, the MDC was applied to the result to indicate the appropriate MI class of either the "left-hand", "right-hand", or "foot" classes. The quadratic Fisher's Discriminant Analysis [9] was used to identify the most appropriate MDC.

F. Fading Feedback Rule

The fading feedback rule was designed to avoid abrupt false classifications. When the selection level was zero, the first classification was defined as the candidate classification. If the last classification was equal to the candidate classification, the selection level was increased; otherwise, the selection level was decreased. When the selection level was equal to N (N=4 per second), the system generated the decisions, such as left, right, and foot. To inform the user of the selection level, the interface system transparentized the arrow and the text to an extent that was proportional to the selection level. During the online test and the real-time experiment, the subjects inspected the feedback sign, which showed the result of the algorithm with the selection level and its classification, as illustrated in Fig. 1. B.

G. Humanoid Robot Control System

A Nao humanoid robot (Aldebran Inc., France) [12] with 25 degrees of freedom was used as the robot platform. The camera on its head transmitted images of the front view to the interface system. To observe the encountered environment and to walk to the target position, five motion commands (e.g., stop, forward walk, body turn, left head turn and right head turn) were programmed. If the body and the head faced the same direction, detection of the "foot" state commanded the robot to walk forward. Because the robot takes a relatively long time to walk, for the convenience of control, the robot was designed to continue walking forward until a "left hand" or "right hand" state was detected. If the head and body faced different directions, the foot event turned the body to be aligned with the head. A "left hand" or "right hand" command stopped the robot if it was walking forward, and continuous left and right events turned the head to the left or the right,

respectively. A left or right turn was achieved by straightening the body after making a left or right turn of the head. It should be noted that our control scheme is different from the state dependent agent-based model [1, 3] because its design was based on postural sensing information and not on environmental conditions.

III. RESULTS

A. Feature Selection

To improve the signal-to-noise ratio and to enhance the classification performance, a time-channel-frequency feature set was selected for each subject as explained in Section II.C. Table I describes the selected feature components of the three subjects.

For the left-hand feature components, the two top-scoring channels over the right sensorimotor cortex (i.e., electrode locations C4, CP4 or FC4) and the frequencies around the alpha (μ) frequency (i.e., 9-15 Hz) were selected. For the right-hand feature components, channels over the left sensorimotor cortex (i.e., electrode locations C3 or FC3) and the frequencies around the alpha (μ) frequency (i.e., 7-16 Hz) were selected. In the experimental setup procedure, the subjects were instructed to imagine movement of one side of the foot. Because subject A chose the right foot and the others chose the left foot, the selected channel locations tended to bias toward the appropriate side. For the foot frequency components, alpha (μ) bands (i.e., 6-14 Hz) and beta bands (i.e., 21-32 Hz) were occupied.

TABLE I
THE RESULT OF FEATURE SELECTION

Subject	Left		Right		Foot	
	Ch	Freq	Ch	Freq	Ch	Freq
A	C4	11-15	C3	12-16	CPz	10-14
	FC4	9-13	FC3	8-12	CP3	21-25
B	FC4	9-13	C3	9-13	FCz	26-30
	C4	10-14	FC3	7-11	FC4	28-32
C	C4	9-13	C3	11-15	CPz	9-13
	CP4	10-14	FC3	11-15	FCz	6-10

B. Performance of the BCI System

Table II-III provides details about the performance of the two hierarchical classifiers for the three subjects. During the first two days, the subjects underwent six sessions of the offline training; one offline training session and one online test are then repeated until the hit ratio of the trained MDC exceeds 75%. Table II shows the number of offline training trials per mental task, the true positive and false positive ratios of the IAC and the accuracy of the MDC for each task. As described in Section II.D, the threshold of the IAC was adjusted to the balanced point so that the sums of the TPR and the FPR of the IAC for all subjects were equal to one. For subject A and C, two and four additional offline training sessions were performed, respectively. After all of the offline training runs, the accuracy was 84.5% for subject A, 87.3%

TABLE II
THE RESULTS OF THE OFFLINE TRAINING

		A	B	C
	Trials	160	120	200
	TPR	0.62	0.66	0.64
	FPR	0.38	0.34	0.36
Accuracy (%)	Left	88.8	96.6	78.5
	Right	89.4	82.0	74.0
	Foot	75.3	83.2	75.0
	Average	84.5	87.3	75.8

TABLE III
THE PERFORMANCE OF THE ONLINE TESTS
USING THE FADING FEEDBACK RULE

		A	B	C
Hit Ratio (%)	Left	80.0	100.0	86.7
	Right	86.7	93.3	66.7
	Foot	73.3	86.7	73.3
	Average	80.0	93.3	75.6
Response Time (sec)	Left	2.83	2.12	2.96
	Right	2.90	2.77	3.38
	Foot	3.65	2.96	3.64
	Average	3.13	2.62	3.32

for subject B and 75.8% for subject C.

To ensure robust classification, the fading feedback rule was applied to the result classifications, and the BCI control performance was directly related to the results from the fading feedback rule. Table III shows the online test performance using the fading feedback rule for the given mental tasks. The response time was the time (in seconds) that was required for the motion commands from the fading feedback rule.

C. Navigation Performance

This section describes the evaluation of the navigation performance of the brain-actuated humanoid robot. The performance was measured by the following metrics:

- 1) *Time*: time in seconds that was required to accomplish the task;
- 2) *Path length*: distance in meters that was traveled to accomplish the task;
- 3) *Way-Point*: the number of waypoints;
- 4) *Collisions*: the number of collisions;

The results are summarized in Table IV. For all subjects, the performance metrics from the manual and BCI experiments was averaged, and the metric values of the BCI control experiment was divided by the manual metrics in the ratio rows. Because all of the subjects were recommended to pass the five waypoints as possible and because the control system and the interface system successfully guided them to navigate the maze, they passed all the five waypoints without any collisions in the manual control scheme. However, although they successfully achieved the goal position during the BCI control experiments, they passed averagely 3.8 waypoints with 0.8 collisions. For the path length, the average path length in the manual experiments was 434.0 cm, and the average path length in the BCI experiments was 423.0 cm; the ratio was 0.99. Because the waypoints were located near to the edge of the maze, the trials that passed all of the

TABLE IV
THE PERFORMANCE OF THE REAL-TIME NAVIGATION CONTROL

Subject	SESSION	Time (s)	Path Length (cm)	Way-points (times /trial)	Collisions (times /trial)
A	Manual	432.7	403.7	5.0	0.0
	BCI	642.4	429.0	4.0	0.7
	Ratio	1.48	1.06	-	-
B	Manual	452.9	389.4	5.0	0.0
	BCI	632.3	430.1	4.7	1.0
	Ratio	1.40	1.10	-	-
C	Manual	424.4	508.9	5.0	0.0
	BCI	448.8	410.0	2.7	0.7
	Ratio	1.06	0.81	-	-
Average	Manual	436.7	434.0	5.0	0.0
	BCI	574.5	423.0	3.8	0.8
	Ratio	1.31	0.99	-	-

waypoints used longer paths than the trials that missed some of the waypoints. For subject C, the average path length of the BCI control experiments was shorter than the path length of the manual control experiment because only an average of 2.7 waypoints was passed. However, for subject B and C, the average number of passed waypoints in the BCI experiments was 4.0 and 4.7, respectively, and the ratio of the path length was 1.06 and 1.10, respectively. Although the averaged path length ratio was 0.99, the average time of the BCI control was 1.31 times longer than the manual control.

IV. CONCLUSION

Although our BCI system is less accurate than the menu-based humanoid robot navigation system [5], it is sufficient to navigate in the indoor environment using the proposed direct-control paradigm. Furthermore, this study introduces the novel humanoid navigation system for controlling a humanoid robot using the low-level motion commands with the asynchronous BCI system. In our control system, subjects were able to command the humanoid robot to position its head at any angle, turn the body to the target angle, and walk to the destination position. As a result, the ratio between the time required for operating the robot by mental control and the time required for manual keyboard control was 1.31. A previous investigation by Millan et al. [1] obtained a ratio of 1.35 with the agent-based model that restricts the motion of robot by environmental states. In our experiments, the travelled distance ratio between the mental and manual controls was an average of approximately 99%. This study introduces the feasibility that a person can control a humanoid robot in a remote place as if he or she was mentally synchronized to the robot. However, because of the number of collisions and passed waypoints showed in Table IV, a more accurate BCI system or a collision avoidance robotic system will be required to control the humanoid robot in real-world. In addition, to represent the more complex function of the humanoid robot besides the navigation, additional mental states are required. The accuracy problem of the BCI system could be resolved by extracting the other informative features (i.e., the adaptive auto-regressive (AAR)

coefficients and the fractal dimensions) and finding the optimal components using optimization methods, such as generic algorithms [13]. Furthermore, the hybrid BCI system that combines the P300 protocol or steady state visually evoked potentials with proposed BCI system could be considered as an alternative system [14]. We also anticipate testing the proposed system with physically disabled people.

REFERENCES

- [1] J. Wolpaw, et al., "Brain-computer interface technology: a review of the first international meeting," *IEEE Transactions on Rehabilitation Engineering*, vol. 8, pp. 164-173, 2000.
- [2] J. Wolpaw, et al., "Brain-computer interfaces for communication and control," *Clinical neurophysiology*, vol. 113, pp. 767-791, 2002.
- [3] J. Millan, et al., "Noninvasive brain-actuated control of a mobile robot by human EEG," *Biomedical Engineering, IEEE Transactions on*, vol. 51, pp. 1026-1033, 2004.
- [4] J. Wolpaw and D. McFarland, "Control of a two-dimensional movement signal by a noninvasive brain-computer interface in humans," *Proceedings of the National Academy of Sciences of the United States of America*, vol. 101, p. 17849, 2004.
- [5] M. Lebedev and M. Nicolelis, "Brain-machine interfaces: past, present and future," *TRENDS in Neurosciences*, vol. 29, pp. 536-546, 2006.
- [6] M. Moore, "Real-world applications for brain-computer interface technology," *Neural Systems and Rehabilitation Engineering, IEEE Transactions on*, vol. 11, pp. 162-165, 2003.
- [7] G. Pfurtscheller, et al., "The hybrid BCI," *Frontiers in Neuroscience*, vol. 4, 2010.
- [8] I. Iturrate, et al., "A noninvasive brain-actuated wheelchair based on a p300 neurophysiological protocol and automated navigation," *Robotics, IEEE Transactions on*, vol. 25, pp. 614-627, 2009.
- [9] B. Rebsamen, et al., "A brain-controlled wheelchair based on P300 and path guidance," 2006, pp. 1101-1106.
- [10] C. Bell, et al., "Control of a humanoid robot by a noninvasive brain-computer interface in humans," *Journal of Neural Engineering*, vol. 5, p. 214, 2008.
- [11] S. Marple Jr, "Digital spectral analysis with applications," 1987.
- [12] T. Dat and C. Guan, "Feature Selection Based on Fisher Ratio and Mutual Information Analyses for Robust Brain Computer Interface," 2007.
- [13] G. McLachlan and J. Wiley, "Discriminant analysis and statistical pattern recognition," 1992.
- [14] L. Parra, et al., "Recipes for the linear analysis of EEG," *NeuroImage*, vol. 28, pp. 326-341, 2005.
- [15] G. Townsend, et al., "Continuous EEG classification during motor imagery-simulation of an asynchronous BCI," *Neural Systems and Rehabilitation Engineering, IEEE Transactions on*, vol. 12, pp. 258-265, 2004.
- [16] D. Gouaillier, et al., "Mechatronic design of NAO humanoid," 2009, pp. 769-774.
R. Boostani, et al., "A comparison approach toward finding the best feature and classifier in cue-based BCI," *Medical and Biological Engineering and Computing*, vol. 45, pp. 403-412, 2007.